Am J Transl Res 2017;9(12):5696-5707
www.ajtr.org /ISSN:1943-8141/AJTR0064440

Original Article

Deep Illumina sequencing reveals differential expression of long non-coding RNAs in hyperoxia induced bronchopulmonary dysplasia in a rat model

Han-Rong Cheng[1,2,3], Shao-Ru He[1,2], Ben-Qing Wu[3], Dong-Cai Li[4], Tian-Yong Hu[4], Li Chen[3], Zhu-Hui Deng[4]

[1]Southern Medical University, Guangzhou 510515, China; [2]Department of Pediatrics, Guangdong General Hospital, Guangdong Academy of Medical Sciences, Guangzhou 510080, China; [3]Department of Pediatrics, Shenzhen People's Hospital, The Second Clinical Medicine College of Jinan University, Shenzhen 518020, Guangdong, China; [4]Longgang ENT Hospital, Institute of ENT and Shenzhen Key Laboratory of ENT, Shenzhen 518172, Guangdong, China

Received May 26, 2017; Accepted November 18, 2017; Epub December 15, 2017; Published December 30, 2017

Abstract: Background: Bronchopulmonary dysplasia (BPD) in premature infants is a predominantly secondary occurrence to intrauterine inflammation/infection and postpartum mechanical ventilation; The purpose of this study is to explore the biological roles of lincRNA in the pathogenesis of BPD. Methods: Newborn rats were randomly assigned to hyperoxia (85% O_2) or the control group: the normoxia group (21% O_2). Lung tissues were collected on days 1-14. The BPD animal model was validated using HE staining, Masson staining, and real-time RT-PCR. Deep Illumina sequencing was used to reveal the differential expression of long non-coding RNAs in hyperoxia bronchopulmonary dysplasia rat models. KEGG and GO functions were predicted. Nine possible BPD-related target lincRNAs were verified by RTq-PCR. Results: The histopathologic changes in lung tissues manifested as hyperaemia, edema, hemorrhage, and inflammation cell infiltration after continuous exposure to hyperoxia for 3 days, and became aggravated after 7 days of hyperoxic exposure. The above lung tissue inflammatory manifestations were alleviated and taken over by pulmonary interstitia hyperplasia and fibrocyte proliferation after 14 days of hyperoxic exposure. The expressions of lincRNA differed between the hyperoxia bronchopulmonary dysplasia model group and the normoxia group. 1175 different lincRNAs were detected in the hyperoxia group and the normoxia group, of which 544 were up-regulated and 631 were down-regulated. 673 moleculars related to GO functions were enriched, including cell location and biological process. Pathway enrichment analysis showed that lincRNA was involved in 257 KEGG pathways. 9 lincRNA were validated in the sample, and the difference was statistically significant. Conclusion: LincRNAs were identified differently between the BPD model and the normoxia group. Many target genes were involved in the developmental process, including cell component biogenesis, biological regulation, transcription regulator, and translation regulator. The BPD might be caused by the activation of the pathways of the EMC-receptor interaction, cytokine-cytokine receptor interaction, cell cycle, and cell adhesion molecules. The present study provides new insight into the pathogenesis mechanism of BPD.

Keywords: lincRNA, microRNA, alveolar development, bronchopulmonary dysplasia, deep Illumina sequencing

Introduction

Preterm infants are born with immature lungs and frequently require respiratory support. Although it is necessary to maintain adequate oxygenation, hyperoxia exposure contributes to the development of chronic lung disease in infancy, also known as bronchopulmonary dysplasia (BPD) [1]. Currently, BPD is defined as requiring supplemental O_2 for > 28 days of life, and/or 36 weeks of corrected gestational age [2]. Pathologically, BPD is characterized by impaired alveolar and vascular development [1]. While preterm infant mortality has decreased over the past 20 years, the incidence of BPD has remained relatively unchanged [3]. Hyperoxia exposure in a newborn rat causes inflammation and alveolar development deficits similar to those seen in infants with BPD [4, 5].

In this study, newborn rats were randomly exposed to room air (21% O_2) or hyperoxia (85% O_2) for 14 days. Our findings suggested that we successfully established rat models of BDP.

Table 1. Real-time PCR primers for genes

Primer	Sequence	(bp)
E-cad	F: 5'-ACAGTCAAACGGCATCTAA	45
	R: 5'-GGTGAAAGCTGGGAAAC	
SPC	F: 5'-GCCAGTTTCGCATTCC	42
	R: 5'-GCTTATAGGCGGTCAGG	
TGF-β	F: 5'-CTGCTGACCCCCACTGATAC	52
	R: 5'-ACGTTTGGGACTGATCCCATT	
N-cad	F: 5'-GACCCAGAAGATGATGTAAG	45
	R: 5'-CTCAGCGTGGATAGGC	
α-SMA	F: 5'-CTTGCTAACGGAGGCG	44
	R: 5'-TCCAGAGTCCAGCACAATA	
β-actin	R: 5'-CGTGCGTGACATTAAAGAG	48
	F: 5'-TTGCCGATAGTGATGACCT	

Deep Illumina sequencing was performed to identify the lincRNAs involved in the BPD. Moreover, differentially expressed lincRNAs between the rat BPD model and the normoxia group were observed. Our study would provide new insights into understanding the mechanism underlying BPD. Consequently, attributing the hidden regulation of lincRNAs is a fascinating new area of research.

Experimental methods

Establishment and validation of high oxygen animal models

Animal model and tissue specimens: A newborn rat model of BPD was used. Two hundred newborn Sprague-Dawley (SD) rats were randomly divided into a model (exposure to hyperoxia [85% O_2] from day of birth) or a control group (exposure to normoxia [21% O_2]). To avoid O_2 toxicity, maternal rats within the model and control groups were switched once every 24 h. Rats were given *ad libitum* access to water and food. On days 1, 3, 7, and 14, after the start of exposure to hyperoxia or normoxia, eight newborn rats from each model or control group were anesthetized by intraperitoneal injection with 5% chloral hydrate, and whole lungs were collected. All specimens were snap-frozen in liquid nitrogen and stored at -80°C until use. Mature SD rats weighing 220-250 g were purchased from the Department of Animals, Experimental Center, Southern Medical University (Guangzhou, China). All animal experiments were approved and supervised by the Ethics Committee of Animals, Shenzhen Peoples' Hospital.

Morphometric analysis

Lungs were fixed with 4% paraformaldehyde and embedded in paraffin. To assess alveolarization, lung sections were stained with H&E and five non-overlapping, representative microphotographs were taken at 400 × magnification by an investigator blinded to the group assignment. A lung injury scoring system was established before the study [6].

The left upper lungs were collected and fixed with xylene, treated with Weigert tulipenin for 5-10 min, and rinsed with water, then stained with Li Chun red acid magenta for 10 min. They were then treated with a phosphomolybdic acid solution for 5 min; an aniline blue dye solution for 5 min; a 1% glacial acetic acid for 1 min; a 95% alcohol dehydration many times; and anhydrous alcohol dehydration and transparent xylene, dried, and sealed with neutral gum.

Real-time PCR

The expressions of E-cad, SPC, TGF-β, N-cad, α-SMA [7, 8] were measured. Total mRNA was extracted from right upper lung lobe tissues after exposure to normoxia or hyperoxia. The real-time PCR was conducted following RNeasy Mini Kit (QIAGEN: 74104) instructions, and real-time PCR (ABI 7500 Fast Real-Time PCR System) was conducted according to kit instructions. Primers were shown in **Table 1**, and β-actin was considered as the standard gene.

RNA isolation, library construction, and sequencing

Right lung lobes were collected from the hyperoxia and noromoxia groups on day 14. Each group included 6 samples. RNA was isolated using the TRIzol reagent (Invitrogen, USA), according to the manufacturer's protocol. RNA concentration was measured using a microscope spectrophotometer (GeneQuant 1300). Agarose gel electrophoresis was applied, and RNA integrity was assessed with the RNA Nano 6000 assay kit (Agilent Technologies, USA). The 1 μg RNA from each sample was used according to the VAHTS Total RNA-seq (H/M/R) Library Prep Kit for Illumina® Kit. The constructed libraries were tested with the Agilent 2100 Bioanalyzer and ABI Step One Plus Real-Time PCR System, and then deep sequenced with the Illumina HiSeqTM2000. The lincRNA sam-

Table 2. The primer sequences for the selected lincRNAs

Primers	Sequence	Length (bp)
GAPDH-F	GCAAGAGAGAGGCCCTCAG	74
GAPDH-R	TGTGAGGGAGATGCTCAGTG	
NONRATT002787.2-F	TGGGAGGAATGTGGGGGTAA	165
NONRATT002787.2-R	CACTCGTGGAAAGGACCACA	
NONRATT003285.2-F	CACGTCCCAAGGCTGTGTTA	117
NONRATT003285.2-R	GGCTACAACCCAAGACAGGG	
NONRATT027300.2-F	GCTTTCCAGAGGACCAGCTT	109
NONRATT027300.2-R	GGGTTATAGGCTGCACTGCT	
NONRATT021010.2-F	TACAGGGACCCAATGCTCTG	186
NONRATT021010.2-R	TCTCATGAGCAAGGGATGGG	
NONRATT012479.2-F	AAAGGCAACTACGCGGAGAG	170
NONRATT012479.2-R	TCCTCATCGTTCCGAATGGC	
NONRATT024319.2-F	TCCTGAGTGAGCTAACCCAA	193
NONRATT024319.2-R	CCTCTCTCTTCCCTGCCAAG	
NONRATT019295.2-F	TAACTGGACTTGCCTGCCTG	155
NONRATT019295.2-R	CGCCCTTCACTCTGGTCATT	
NONRATT011393.2-F	CACCGTGCCTAAAGATGGTG	232
NONRATT011393.2-R	TGGTAGAGGAAGCAAGGTGG	
NONRATT022113.2-F	TTGCCATCTAGCAGCGAACT	106
NONRATT022113.2-R	AGCACCTGCTGATCAAATGGA	

ples were subjected to PE150 sequencing according to the HiSeq 3000/4000 PE Cluster Kit instructions and the Hiseq4000 sequencer operating instructions. This data was used in the following analysis to detect gene expression, variable splicing, new transcript prediction and annotation, and gene fusion based on the quality control (QC) established before the studies [2, 4, 9-14].

Validation of the lincRNAs using real-time PCR

In this study, lung tissues were collected from high-oxygen BPD animal models and the normoxia group. According to the criteria (different expressions, FDR<0.001, gene length no more than 2 kb, KEGG, and GO pathways), we selected seven BPD-related target lincRNA, and the primers were shown in **Table 2**.

Statistical analysis

All data are presented as mean (X) ± standard deviation (SD). SPSS13.0 software was used for statistical analysis. Inter-group comparisons were conducted using t-tests and multiple group comparisons using one-way analysis of variance (ANOVA). $P<0.05$ suggests a statistically significant difference.

Results

Establishment and validation of hyperoxia BPD rats animal model

As shown in **Figure 1A**, the body weight of the rats was significantly lower in the hyperoxia group than in the aerial group. The differences between the two groups were statistically significant on days 3, 7, 10 and 14, respectively ($P<0.05$).

As shown in **Figure 1B**, all 85% O_2-exposed rats showed significant deficits in alveolar development. HE staining results revealed that they showed congestion, edema, bleeding, and inflammatory cell infiltration on day 3, and more obviously on day 7 with hyperoxia, congestion edema, interstitial thickening, fibroblast proliferation on the 14th day. The differences in lung injury scoring were statistically significant ($P<0.05$) (**Figure 1C**). Masson staining results suggested that the deposition of blue collagen increased in the lung tissue of the hyperoxia group with the prolongation of time, while only a small amount of blue collagen was distributed around the bronchial wall and the blood vessel in the control group (**Figure 1D**).

Real-Time PCR showed that the expression of SPC and E-cad decreased with the prolongation of hyperoxia exposure compared with the normoxia group, while the expression of TGF-β, N-cad and α-SMA increased with the prolongation of hyperoxia exposure (**Figure 2**).

Results of deep Illumina sequencing

In the hyperoxia group, there were 30225 gene expressions associated with the lincRNA; there were 30361 gene expressions related to lincRNA in the normoxia group, as shown in **Table 3**.

To identify the lincRNAs involved in the BPD, the expression profiles of the lincRNAs were examined on day 14. The expression of lincRNA was different between the hyperoxia bronchopulmonary dysplasia model and the normoxia group. 1175 different lincRNAs were detected in the hyperoxia group and the normoxia group,

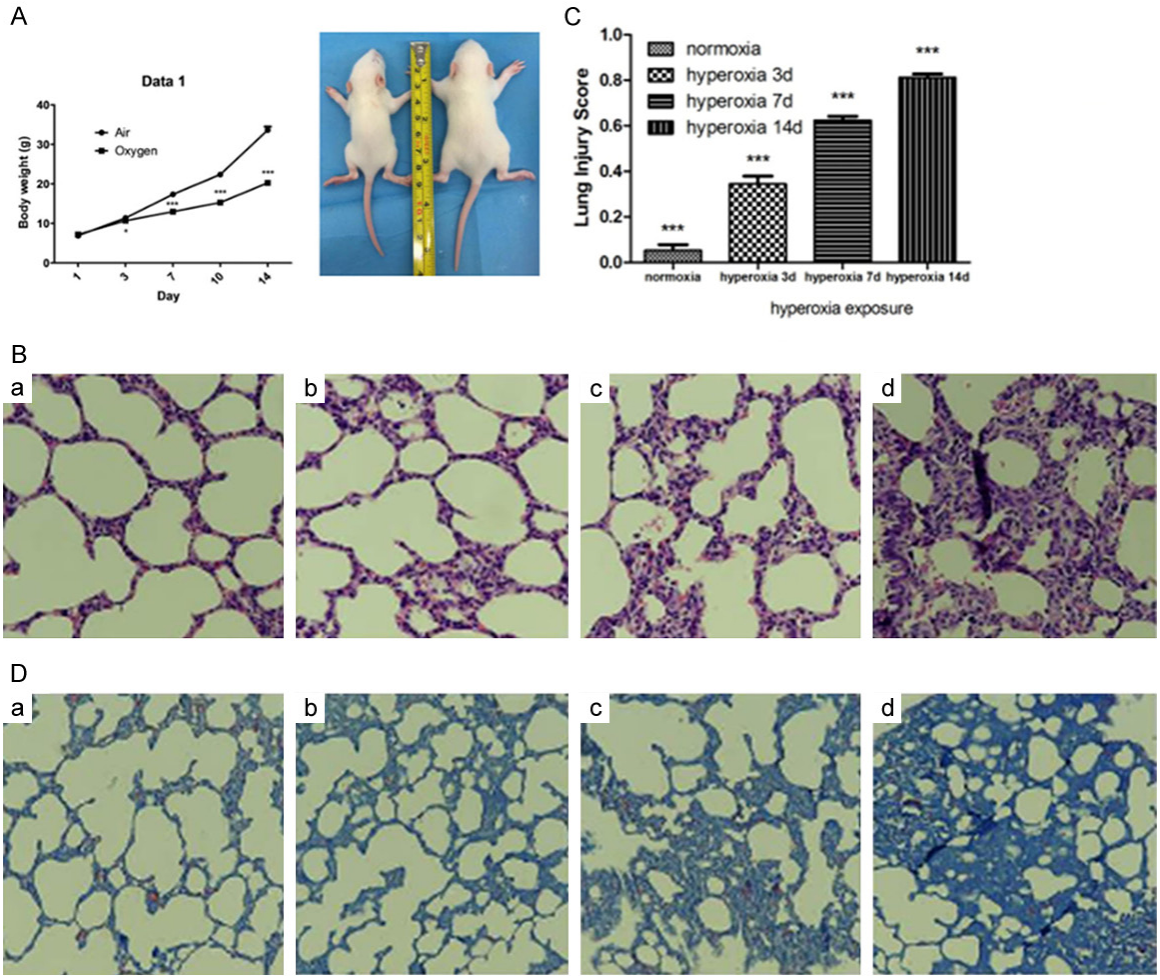

Figure 1. The changes of rats' weight and lung histology between two groups. A: The weight (g) of normoxia group and hyperoxia group rats after birth. B: The pathological change of lung tissues during exposed to hyperoxia (HEstain × 400). a: Normoxia. b: Hyperoxia 3 d. c: Hyperoxia 7 d. d: Hyperoxia 14 d. C: Lung histology shows levels of lung injury after different days of hyperoxia exposure. The lung injury scoring of the hyperoxia group was significantly higher than that of the aerial group. The difference of lung injury scoring was statistically significant at 3, 7, 10 and 14, compared to normoxia group respectively. (P<0.05). D: The pathological change of lung tissues during exposed to hyperoxia (Masson stain × 400). Compared with the normoxia group, the alveolar epithelial cells were swollen in the hyperoxia group, and the alveolar cavity was filled with massive exudate, interstitial congestion, edema and inflammatory cells, but the alveolar structure was still complete at 3 days. At 7 days, the alveolar wall of high oxygen group thicken, interstitial congestion and edema is more obvious; At 14 days, the pulmonary inflammatory exudation and edema decreased, interstitial thickened significantly, hyperplasia of fibroblast, and alveolar fused while the number decreased, and lung tissue become disorder. a: lung tissue of normoxia group: a small amount of blue collagen distributed around the bronchial wall and blood vessels. b: lung tissue of hyperoxia 3 d, the blue collagen increase around the bronchial wall and blood vessels. c: lung tissue of hyperoxia 7 d, interstitial collagen increased. d: lung tissue of hyperxia 14 d, more blue collagen deposition in the interstitial tissue.

out of which 544 were up-regulated and 631 were down-regulated. Here, the differential expression gene was defined as a gene with FDR ≤ 0.001 if its fold change is more than 2-fold. **Table 4** shows parts of the differential expression analysis, and **Figure 3** shows the distribution of all genes in the sequenced samples.

GO enrichment analyses

GO enrichment analyses were performed in order to investigate the possible roles of the target genes. Most of the GO terms belonged to the biological process category, suggesting the occurrence of a series of molecular events in BPD. 673 molecular functions were enriched

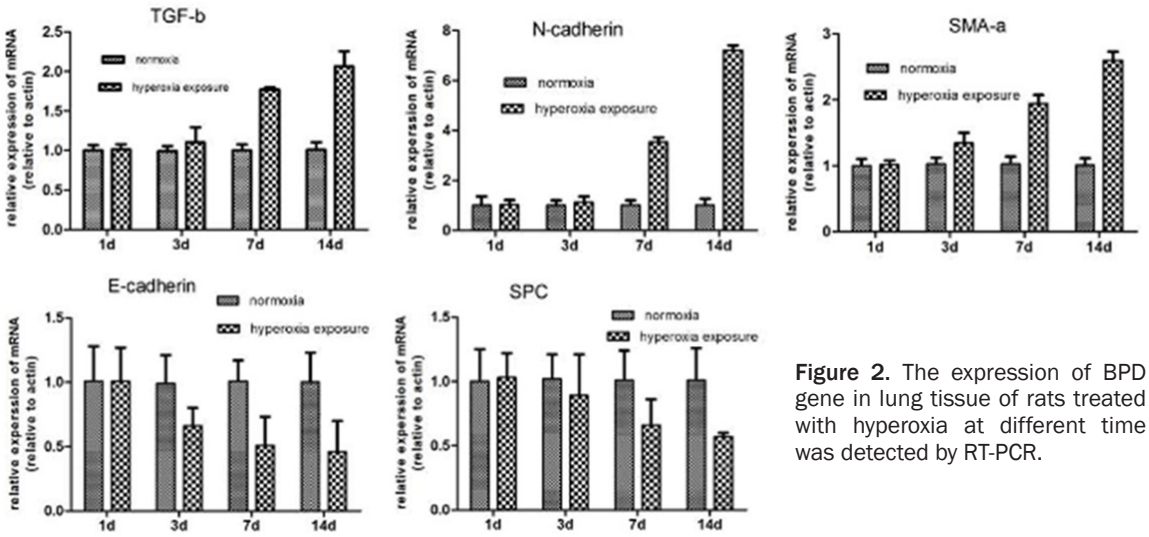

Figure 2. The expression of BPD gene in lung tissue of rats treated with hyperoxia at different time was detected by RT-PCR.

Table 3. lincRNA gene expression in the hyperoxia group (RPKM)

GeneID	Uniq_reads_num (8496256)	Length	Coverage	RPKM
Macf1	84087	23521	0.991	420.7706964
Ahnak	64659	17592	0.999	432.5996639
Col3a1	59550	4769	0.9973	1469.693772
Fn1	58105	8331	0.9978	820.8972134
NONRATT003468.2	51801	2431	0.9938	2507.988815
Eef1a1	49069	1730	0.9931	3338.362664
Eln	45581	3590	1	1494.382629
NONRATT003466.2	41231	885	0.9989	5483.438889

by GO, including cell location and biological process. The details of the GO terms are shown in the differential expression gene GO function classification chart. The distribution of GO gene functional groups was used to visually reflect the distribution of differential genes in GOTerm, which is rich in biological processes (BP), cellular components (CC), and molecular functions (MF). Classification of differentially expressed genes is shown in **Figure 4**, and **Table 5** shows part of the GO enrichment analysis of differentially expressed genes between the hyperoxia group sample and the normoxia group sample. The abscissa represented the GO Term enriched in three ontologies, and the ordinate indicates the number and proportion of genes enriched on the GO Term.

KEGG enrichment analyses

KEGG enrichment analyses were performed to investigate the possible roles of the target genes. Pathway enrichment analysis showed that lincRNA was involved in 257 KEGG pathways. The results showed that the enriched KEGG terms were associated with ECM-receptor interaction, cell cycle, CAMs, and cytokine-cytokin receptor interaction. The top 20 enriched KEGG terms of the target genes are listed in a scatter plot (**Figure 5**), and **Table 6** shows parts of the results of the KEGG Pathway enrichment analysis.

Variable shear analysis

Multiple mRNA transcripts were produced by a gene because of variable splicing. Different mRNAs may be translated into different proteins [20]. Although variable splicing is known to be ubiquitous in eukaryotes, we may still underestimate its proportion. *In vivo*, there are seven types of variable splicing: A) Exon skipping; B) Intron retention; C) Alternative 5' splice site; D) Alternative 3' splice site; E) Alternative first Exon; F) Alternative last Exon; G) Mutually exclusive Exon.

Alternative splicing events and gene statistics of the hyperopia and normoxia group are as follows: (**Figure 6A**, **6B**).

New transcripts prediction of lncRNA

There were 9816 new transcripts predicted of LncRNA in the hyperoxia group and 13098 new

Table 4. Differentially expression of lincRNAs between normoxia and hyperoxia group

GeneID	Normoxia (raw)	Hyperoxia (raw)	Normoxia (normalized)	Hyperoxia (normalized)	Fold change (hyperoxia/ normoxia)	Up/Down (hyperoxia/ normoxia)	*P*-value	FDR
NONRATT032639.1	3	114	0.150207951	6.054907399	40.3101658	Up	5.74E-32	4.11E-30
Slc26a4	2	51	0.077780306	2.103976161	27.05024284	Up	3.68E-14	9.93E-13
Ptgs2	19	386	1.161497807	25.03128158	21.55086426	Up	4.00E-95	1.01E-92
Gdf15	11	201	1.338256216	25.94021847	19.38359647	Up	4.10E-49	4.68E-47
Ptprv	4	73	0.081493651	1.577675326	19.35948752	Up	1.22E-18	4.58E-17
NONRATT020346.2	15	222	3.403484856	53.43385723	15.69974878	Up	2.04E-51	2.49E-49
NONRATT006034.2	2	29	0.580908934	8.935256937	15.38151063	Up	1.06E-07	1.44E-06
Mt2A	3	43	0.8690883	13.21423701	15.20471166	Up	7.17E-11	1.44E-09
Apod	2	26	0.261683034	3.608692742	13.79031988	Up	7.64E-07	9.03E-06

(1) geneSymbol: name of gene; (2) normoxia (raw): the UniqReads match to the gene in Normoxia group; (3) hyperoxia (raw): the UniqReads match to the gene in Hyperoxia group; (4) Fold change (hyperoxia/normoxia): differential expression folds; (5) Up/Down (hyperoxia/normoxia): hyperoxia group compare to normoxia group is up or down; (6) *P*-value: Differences in the *P* value test; (7) FDR: False Discovery Rate, is a correction method of difference test.

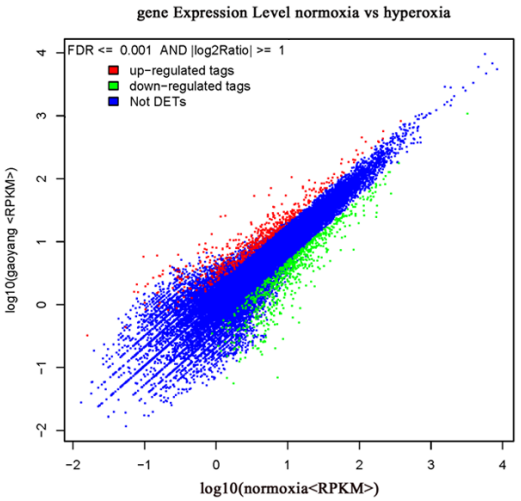

Figure 3. The distribution of all genes in the sequenced samples. The abscissa indicates the expression of the control sample (logarithm), and the ordinate indicates the expression of the treated sample (logarithmic). Each point in the figure represents a gene, and the red and green dots represent a significant expression of the gene. The red dot indicates that the gene expression is upregulated (treated sample relative to control sample). The green point indicates that the gene expression level is downregulated (treated sample relative to control sample). The blue dots indicate that these genes are not significantly different.

transcripts predicted of LncRNA in the normoxia group. **Table 7** shows parts of the results of the new transcripts predicted of LncRNA.

Confirmation of lincRNAs by using RTqPCR analysis

9 lincRNAs were selected for the RT-qPCR analysis. These lincRNAs are NONRATT002787.2, NONRATT003285.2, NONRATT027300.2, NONRATT021010.2, NONRATT012479.2, NONRATT024319.2, NONRATT019295.2, NONRATT011393.2 and NONRATT022113.2.

The relative expressions of the lincRNAs in different groups were calculated as the ratio of the gene expression levels relative to GAPDH. For most of the examined lincRNAs, the expression patterns identified using qPCR were similar to those obtained using the RNA-seq analyses, although the relative expression levels were not completely consistent. Our results showed that NONRATT002787.2, NONRATT003285.2, and NONRATT012479.2 were up-regulated, and NONRATT024319.2, NONRATT019295.2, NONRATT011393.2, and NONRATT022113.2 were down-regulated when the hyperoxia sample is compared to the normoxia group, which is consistent with the RNA-seq data. Both NONRATT027300.2 and NONRATT021010.2 were predicted to up-regulate in the RNA-seq, but the qPCR showed down-regulation (**Figure 7**).

Discussion

Bronchopulmonary dysplasia (BPD) is a common, chronic lung disease in infants, frequently seen in premature newborns with low fetal age and birth weight with a complicated pathogenesis. Supraphysiological O_2 concentrations, mechanical ventilation, and inflammation significantly contribute to the development of bronchopulmonary dysplasia (BPD). Exposure of newborn rats to hyperoxia causes inflammation and impaired alveolarization similar to that seen in infants with BPD [15].

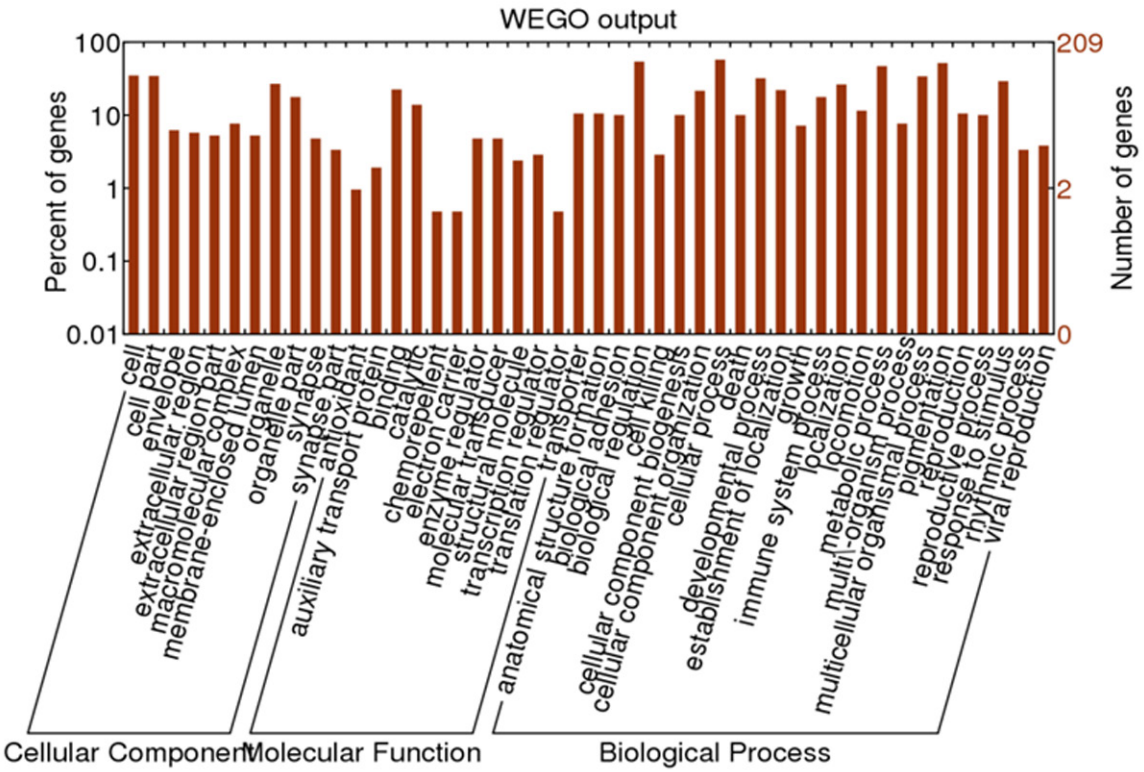

Figure 4. Classification of differentially expressed genes.

Table 5. GO enrichment analysis of differentially expressed genes between hyperoxia group sample and normoxia group sample

Term	ID	Input number	Background number	*P*-value	Corrected *P*-value
Cell proliferation	GO:0008283	122	1446	9.73E-05	cell proliferation
Cell cycle	GO:0007049	83	902	9.78E-05	cell cycle
Regulation of cell proliferation	GO:0042127	103	1180	0.000103418	regulation of cell proliferation
Response to oxidative stress	GO:0006979	41	359	0.000110927	response to oxidative stress
Response to oxygen-containing compound	GO:1901700	123	1424	3.70E-05	response to oxygen-containing compound
Cellular response to fibroblast growth factor stimulus	GO:0044344	15	86	0.000412377	cellular response to fibroblast growth factor stimulus

(1) Term: description information of Gene Ontology function; (2) ID: enriched GO ID; (3) Input number: the number of genes associated with the Term; (4) Background number: The number of genes associated with the Term in all background genes; (5) *P*-Value: statistically significant level of enrichment analysis; (6) Corrected *P*-Value: *P*-value after Bonferroni correction.

The body weight of the O_2 rats was slightly lower than that of the normoxic rats on day 3, but was markedly lower than normoxic rats on days 7 and 14. The difference in lung injury scoring was statistically significant on days 3, 7, 10 and 14 compared to the normoxia group, respectively ($P<0.05$). Prolonged hyperoxia caused substantial alterations in lung morphology. Newborn BPD rat lung tissues displayed enlarged alveolar spaces, thickened pulmonary septa, a simplified alveolar structure, and higher lung injury scoring that was reduced in comparison to room air-exposed controls. In terms of the Masson stain, the rats exposed to prolonged hyperoxia showed an increase in the blue collagen deposition in the interstitial tissue compared to room air-exposed controls. All results indicated a pulmonary developmental disorder.

Gene expressions of several well-known BPD biomarkers were measured with Real-time

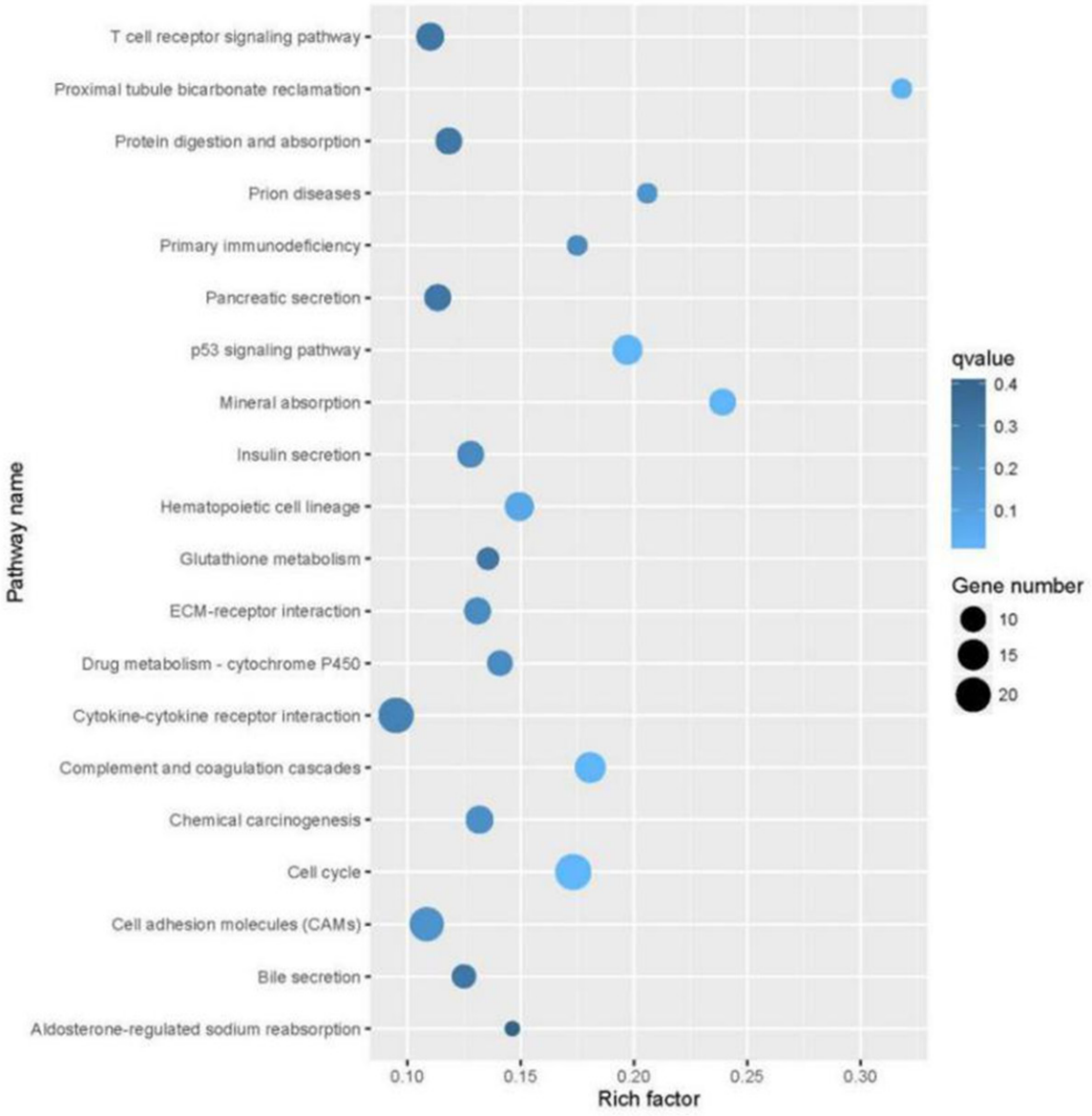

Figure 5. Kegg enrichment analysis Scatter plot of differential gene expression. Rich Factor is the proportion of the genes that indicate the difference to the pathway term to the genes that are annotated to the Pathway. Q value is the correction of *P* value, its value is 0~1. The vertical axis represents the Pathway items, and the abscissa indicates the Rich factor. The point indicates the expressed genes which is significant difference, the size of the dots indicates a in the number of expressed genes which is significant difference. The larger the point, the greater number of genes significantly differentially expressed. Points of different colors represent different Q values.

PCR. The expression of SPC and E-cad mRNA decreased with the prolongation of hyperoxia exposure, while the expression of TGF-β, N-cad and α-SMA increased with the prolongation of hyperoxia exposure. Transforming growth factor (TGF)-β signaling is involved in pulmonary fibrosis and the inhibition of branching morphogenesis in lung development. TGF-β mRNA was increased 2-fold in hyperoxia-induced BPD rats on 14 d. N-cad, an interstitial cell marker, was dramatically increased 7.2-fold on 14 d. The α-SMA is one of the six actin families; it is expressed in myofibroblasts, and its expression increased 2.6-fold on 14 d. SPC is a specific marker of lung epithelial type II cells, which reduced by 43% in the lungs of O_2 treated rats. E-cad, a classic epithelial cell marker, had decreased by 54% in hyperoxia-induced BPD

Table 6. Results of differentially expressed genes Pathway enrichment analysis between hyperoxia and normoxia group

Term	ID	Input number	Background number	*P*-value	FDR
Cell cycle	rno04110	22	127	8.08E-06	0.002076
ECM-receptor interaction	rno04512	11	84	0.009567471	0.208417679
Cell adhesion molecules (CAMs)	rno04514	19	175	0.005504154	0.17682094
Cytokine-cytokine receptor interaction	rno04060	21	221	0.013814826	0.253600731
Apoptosis	rno04210	13	141	0.054691345	0.488033392
cAMP signaling pathway	rno04024	15	196	0.12890285	0.767890039

(1) Term: Name of Signal path; (2) ID: enriched pathway matched to the ID of KEGG database; (3) Input number: the number of differentially expressed genes that locate on the pathway; (4) Background number: the number of genes associated with this pathway; (5) *P*-value: significance level of the pathway enrichment; (6) FDR: multiple test correction for *P*-value.

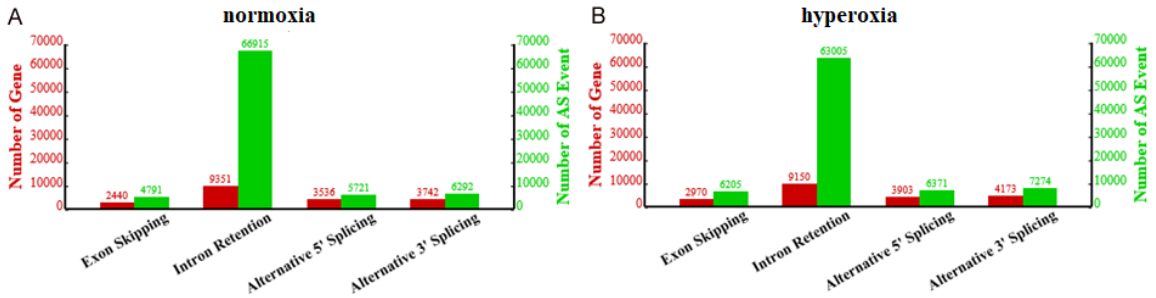

Figure 6. Variable shear event statistics of mRNA between two groups. A: Variable shear event statistics of normoxia sample mRNA. The label represents a variable shear event, and the ordinate represents the number of genes or the number of variable shear events. B: Variable shear event statistics of hyperoxia sample mRNA. The label represents a variable shear event, and the ordinate represents the number of genes or the number of variable shear events.

rats on day 14. These results indicate that hyperoxia can cause BPD in the lungs of rats.

Taken together, these biomarker changes, accompanied by pulmonary morphological changes, are consistent with the development of human BPD. We successfully established and validated rat models of hyperoxia BPD. This is consistent with previous studies [8, 16, 17].

It is now becoming evident that ncRNAs are responsible for many aspects of gene regulation. LincRNAs, which are involved in chromatin remodeling, act as transcription co-factors, and there are competing endogenous RNA hypotheses for lincRNAs. Furthermore, LincRNAs act as evolutionary reservoirs [18, 19]. However, long noncoding RNAs (lncRNAs) remain relatively unexplored due to the challenges of computational prediction under poor sequence conservation and low homology within the set of lncRNAs. Some of these challenges have been addressed by revolutionary next-generation sequencing (NGS) inventions such as RNA-Seq, which captures whole transcriptome data, including lncRNAs [20-22].

Our study showed that prolonged hyperoxia alters lincRNA expression in the neonatal rat lung. In the hyperoxia group, there are 30225 gene expressions associated with the lincRNA, and there are 30361 gene expressions related to lincRNA in the normoxia group. Using a rigorous standard for the selection of differential expressions, we found that the expression of lincRNA between hyperoxia bronchopulmonary dysplasia model and the normoxia group was different. A total of 1175 different lincRNAs were detected in the hyperoxia group and the normoxia group, among which 544 were up-regulated and 631 were down-regulated. Deep Illumina sequencing results revealed that the differential expression of long non-coding RNAs in hyperoxia induced bronchopulmonary dysplasia in a rat model.

Gene Ontology (GO) could describe this molecular function, including cellular components

Table 7. New Transcription Information of LncRNA_ form hyperoxia group

Novel_TU_ID	Chromosome	+/-	Blocks	Sizes	Starts
NovelTr_1	chr1	+	1	576	1549500
NovelTr_2	chr1	-	5	143,144,264,261,88	14,548,671,455,595,100,000,000,000,000,000,000
NovelTr_3	chr1	-	5	97,179,258,243,256	16,581,261,659,633,100,000,000,000,000,000,000
NovelTr_4	chr1	-	3	478,243,256	166,044,116,611,731,000,000

Header description: (1) Novel_TU_ID: ID of new transcript; (2) Chromosome: the chromosome belonged to; (3) +/-: positive or negative chain information of the chromosome in the new transcript; (4) Blocks: the exon of new transcripts; (5) Sizes: each exon size (comma separated) of new transcriptions; (6) Starts: the location of each exon's start site on the chromosome (comma separated).

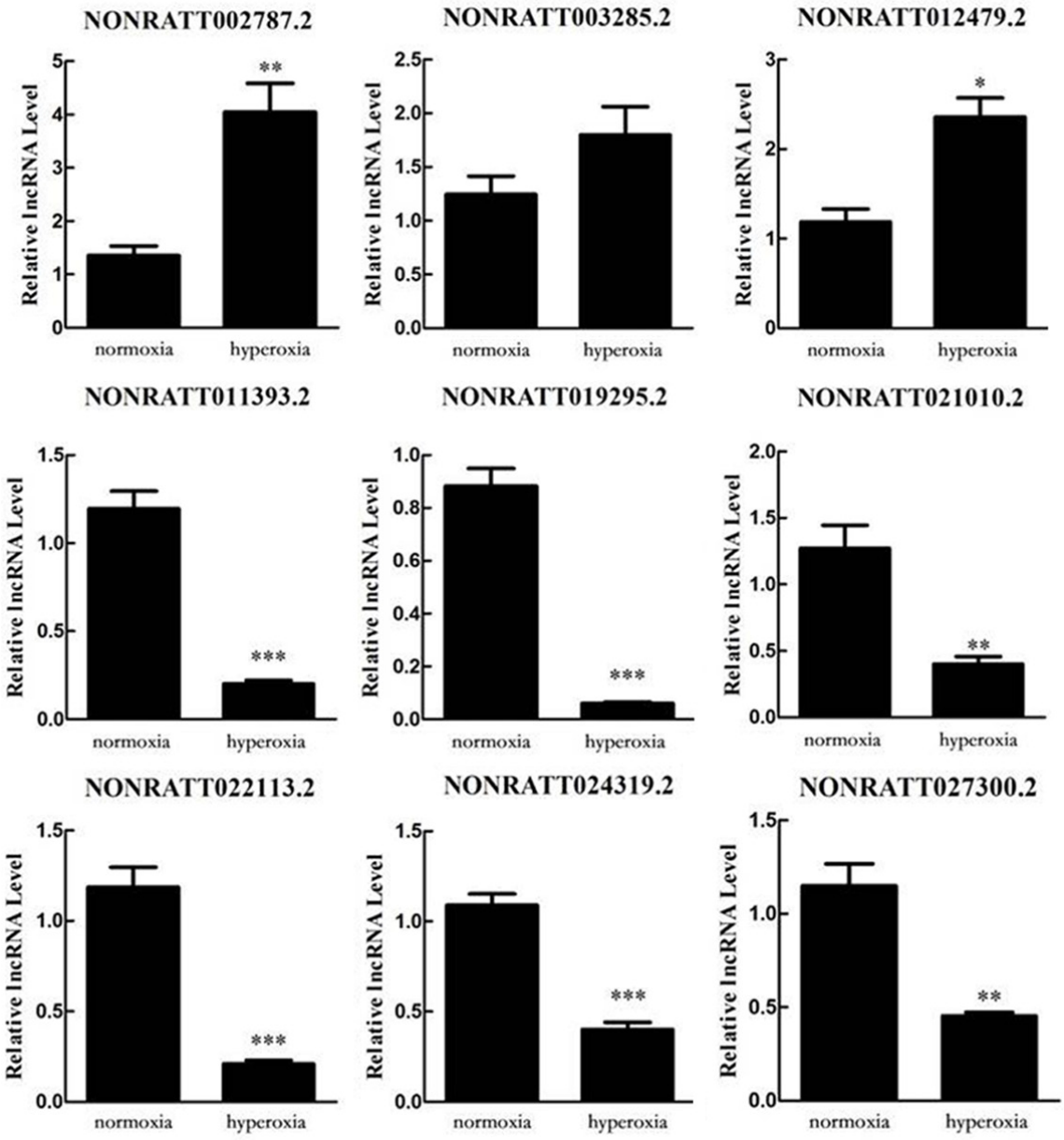

Figure 7. RT-PCR analysis of 9 lincRNAs relative expression.

and biological processes [23]. GO enrichment analysis revealed that most of the GO terms belonged to the biological process category, suggesting the occurrence of a series of molecular events in BPD. A total of 673 molecular functions were enriched by GO, including cell

location and biological process. The details of the GO terms are shown in the differential expression gene GO function classification chart. KEGG (the main pathway associated with the public database) is used for metabolic pathway enrichment analysis of differentially expressed genes [24]. Pathway enrichment analysis showed that lincRNA was involved in 257 KEGG pathways. These results showed that enriched KEGG terms are associated with ECM-receptor interaction, cell cycle, CAMs and cytokine-cytokin receptor interaction. The top 20 enriched KEGG terms of the target genes are listed in a scatter plot. Interestingly, many of the genes could be targeted by one lincRNA, such as NONRATT022113.2, NONRATT011393.2, NONRATT019295.2, NONRATT024319.2, NONRATT021010.2, NONRATT027300.2, NONRATT003285.2 and NONRATT002787.2. The fact that one lincRNA targets many genes may suggest that lincRNA may be involved in a series of biological processes. Previous studies have also shown that some linRNAs are involved in many biological events [25]. Therefore, we hypothesized a correlation between the BPD and these GO terms or pathways.

Variable shear analysis shows that there are 9816 new transcripts predicted of LncRNA from the hyperoxia group, and 13098 new transcripts predicted of LncRNA from the normoxia group. Therefore, lincRNA is involved in the regulation of the transcription processes during the development of BPD. The prediction of BPD new transcripts in this study is an important complement to a comprehensive understanding of the pathogenesis of BPD.

Conclusion

Overall, LincRNA may be involved in the development of BPD, not only in post-transcriptional regulation, but also in the regulation of the transcription processes. This study provides new insight into the biological processes of BPD.

Acknowledgements

This work was supported by grant from the Shenzhen science and technology innovation projecr of China (JCYJ20140416122812046).

Disclosure of conflict of interest

None.

Address correspondence to: Shao-Ru He, Southern Medical University, Guangzhou 510515, China; Department of Pediatrics, Guangdong General Hospital, Guangdong Academy of Medical Sciences, Guangzhou 510080, China. Tel: +86-13510099301; Fax: +86-13510099301; E-mail: hsr1605@126.com; Ben-Qing Wu, Department of Pediatrics, Shenzhen People's Hospital, The Second Clinical Medicine College of Jinan University, Shenzhen Guangdong 518020, China. E-mail: wubenqing783@126.com

References

[1] Kobaly K, Schluchter M, Minich N, Friedman H, Taylor HG, Wilson-Costello D, Hack M. Outcomes of extremely low birth weight (<1 kg) and extremely low gestational age (<28 weeks) infants with bronchopulmonary dysplasia: effects of practice changes in 2000 to 2003. Pediatrics 2008; 121: 73-81.

[2] Ali Z, Schmidt P, Dodd J, Jeppesen DL. Bronchopulmonary dysplasia: a review. Arch Gynecol Obstet 2013; 288: 325-333.

[3] Niedermaier S, Hilgendorff A. Bronchopulmonary dysplasia - an overview about pathophysiologic concepts. Mol Cell Pediatr 2015; 2: 2.

[4] Choi CW, Lee J, Lee HJ, Park HS, Chun YS and Kim BI. Deferoxamine improves alveolar and pulmonary vascular development by upregulating hypoxia-inducible factor-1α in a rat model of bronchopulmonary dysplasia. J Korean Med Sci 2015; 30: 1295-1301.

[5] Zhu Y, Fu J, Yang H, Pan Y, Yao L, Xue X. Hyperoxia-induced methylation decreases RUNX3 in a newborn rat model of bronchopulmonary dysplasia. Respir Res 2015; 16: 75.

[6] You K, Xu X, Fu J, Xu S, Yue X, Yu Z, Xue X. Hyperoxia disrupts pulmonary epithelial barrier in newborn rats via the deterioration of occludin and ZO-1. Respir Res 2012; 13: 36.

[7] Chen X, Xiao W, Wang W, Luo L, Ye S, Liu Y. The complex interplay between ERK1/2, TGF/Smad, and jagged/notch signaling pathways in the regulation of epithelial-mesenchymal transition in retinal pigment epithelium cells. PLoS One 2014; 9: e96365.

[8] Yang H, Fu J, Xue X, Yao L, Qiao L, Hou A, Jin L, Xing Y. Epithelial-mesenchymal transitions in bronchopulmonary dysplasia of newborn rats. Pediatr Pulmonol 2014; 49: 1112-1123.

[9] Cock PJ, Fields CJ, Goto N, Heuer ML, Rice PM. The Sanger FASTQ file format for sequences with quality scores, and the Solexa/Illumina FASTQ variants. Nucleic Acids Res 2010; 38: 1767-1771.

[10] Kim D, Pertea G, Trapnell C, Pimentel H, Kelley R, Salzberg SL. TopHat2: accurate alignment

of transcriptomes in the presence of insertions, deletions and gene fusions. Genome Biol 2013, 14: R36.
[11] Mortazavi A, Williams BA, McCue K, Schaeffer L and Wold B. Mapping and quantifying mammalian transcriptomes by RNA-Seq. Nat Methods 2008; 5: 621-628.
[12] Audic S and Claverie JM. The significance of digital gene expression profiles. Genome Res 1997; 7: 986-995.
[13] Wang Z, Gerstein M and Snyder M. RNA-Seq: a revolutionary tool for transcriptomics. Nat Rev Genet 2009; 10: 57-63.
[14] Trembath A and Laughon MM. Predictors of bronchopulmonary dysplasia. Clin Perinatol 2012; 39: 585-601.
[15] Jackson W, Laughon MM. Biomarkers of bronchopulmonary dysplasia. Bronchopulmonary dysplasia. Springer International Publishing 2016.
[16] Alejandre-Alcázar MA, Kwapiszewska G, Reiss I, Amarie OV, Marsh LM, Sevilla-Pérez J, Wygrecka M, Eul B, Köbrich S, Hesse M, Schermuly RT, Seeger W, Eickelberg O, Morty RE. Hyperoxia modulates TGF-beta/BMP signaling in a mouse model of bronchopulmonary dysplasia. Am J Physiol Lung Cell Mol Physiol 2007; 292: L537-L549.
[17] Sauvageau M, Goff LA, Lodato S, Bonev B, Groff AF, Gerhardinger C, Sanchez-Gomez DB, Hacisuleyman E, Li E, Spence M, Liapis SC, Mallard W, Morse M, Swerdel MR, D'Ecclessis MF, Moore JC, Lai V, Gong G, Yancopoulos GD, Frendewey D, Kellis M, Hart RP, Valenzuela DM, Arlotta P, Rinn JL. Multiple knockout mouse models reveal lincRNAs are required for life and brain development. Elife 2013; 2: e01749-e01749.
[18] Khalil AM, Guttman M, Huarte M, Garber M, Raj A, Rivea Morales D, Thomas K, Presser A, Bernstein BE, van Oudenaarden A, Regev A, Lander ES, Rinn JL. Many human large intergenic noncoding RNAs associate with chromatin-modifying complexes and affect gene expression. Proc Natl Acad Sci U S A 2009; 106: 11667-11672.
[19] Ching T, Masaki J, Weirather J, Garmire LX. Non-coding yet non-trivial: a review on the computational genomics of lincRNAs. Bio Data Min 2015; 8: 44.
[20] Volders PJ, Verheggen K, Menschaert G, Vandepoele K, Martens L, Vandesompele J, Mestdagh P. An update on LNCipedia: a database for annotated human lncRNA sequences. Nucleic Acids Res 2015; 43: 174-180.
[21] Zhu QL, Shi L, Peng G. High-throughput sequencing technology and its application. J North Agricult Univ 2014; 21: 84-96.
[22] Wikipedia F, Ontology G, Go E, Consortium GO, Ontology TG, Go E. Gene ontology. 2014.
[23] Ooi HS, Schneider G, Lim TT, Chan YL, Eisenhaber B, Eisenhaber F. Biomolecular pathway databases. Methods Mol Biol 2010; 609: 129-144.
[24] Xie H, Ma H, Zhou D. Plasma HULC as a promising novel biomarker for the detection of hepatocellular carcinoma. Biomed Res Int 2013; 2013: 136106.
[25] Loewen G, Zhuo Y, Zhuang Y, Jayawickramarajah J, Shan B. lincRNA HOTAIR as a novel promoter of cancer progression. J Can Res Updates 2014; 3: 134-140.